An Efficient PML Implementation for the ADI-FDTD Method

Shumin Wang and Fernando L. Teixeira

***Abstract*—A novel implementation of the perfectly matched layer (PML) absorber for the alternating-direction implicit finite-difference time-domain method is proposed and implemented. It is shown that, compared to the traditional PML implementation, the performance of the proposed PML is more efficient for large Courant numbers.**

***Index Terms*—Alternating-direction implicit (ADI) method, finite-difference time-domain (FDTD) method, perfectly matched layer (PML).**

I. Introduction

THE ALTERNATING-DIRECTION implicit finite-difference time-domain (ADI-FDTD) method [1]–[4] is an attractive alternative to the standard FDTD due to its unconditional stability with moderate computational overhead. The ADI-FDTD can be particularly useful for problems involving devices with fine geometric features that are much smaller than the wavelengths of interest. In order to be applied for unbounded domain problems, the ADI-FDTD requires the use of appropriate absorbing boundary conditions, such as the perfectly matched layer (PML) [5]–[8]. The PML has been first extended to the ADI-FDTD method in [9], where it has been shown that while the PML can still provide very small reflections at small Courant numbers, its performance deteriorates for large Courant numbers.

Because the ADI-FDTD method is most necessary for large (greater than unity) Courant numbers (as long as the accuracy of the results is not impacted by the potential increase on the time step truncation error [4]), a PML implementation that does not deteriorate for large Courant numbers is highly desirable. In this letter, we introduce a novel PML implementation for the ADI-FDTD for this purpose. For simplicity, we consider a two-dimensional (2-D) TE problem, but the basic approach equally applies to the three-dimensional (3-D) problem.

II. ADI-FDTD Update Equations With PML

In the split-field PML formulation [5], the E_x, E_y, H_{zx} and H_{zy} field components satisfy the following relations:

$$\epsilon_0 \frac{\partial E_x}{\partial t} + \sigma_y E_x = \frac{\partial (H_{zx}+H_{zy})}{\partial y} \tag{1}$$

$$\epsilon_0 \frac{\partial E_y}{\partial t} + \sigma_x E_y = -\frac{\partial (H_{zx}+H_{zy})}{\partial x} \tag{2}$$

$$\mu_0 \frac{\partial H_{zx}}{\partial t} + \frac{\sigma_x}{\epsilon_0} H_{zx} = -\frac{\partial E_y}{\partial x} \tag{3}$$

$$\mu_0 \frac{\partial H_{zy}}{\partial t} + \frac{\sigma_y}{\epsilon_0} H_{zy} = \frac{\partial E_x}{\partial y}. \tag{4}$$

In the ADI-FDTD method, the update at each time step is divided into two sub-steps. First, assuming that E_y is computed implicitly at the time step $(n+(1/2))$, (1)–(4) are discretized as [2], [9]

$$\begin{aligned} E_x^{n+(1/2)}&\left(i+\tfrac{1}{2}, j\right) \\ &= \alpha_x^e\left(i+\tfrac{1}{2}, j\right) E_x^n\left(i+\tfrac{1}{2}, j\right) + \beta_x^e\left(i+\tfrac{1}{2}, j\right) \\ &\quad \cdot \left[H_{zx}^n\left(i+\tfrac{1}{2}, j+\tfrac{1}{2}\right) - H_{zx}^n\left(i+\tfrac{1}{2}, j-\tfrac{1}{2}\right)\right. \\ &\quad \left. + H_{zy}^n\left(i+\tfrac{1}{2}, j+\tfrac{1}{2}\right) - H_{zy}^n\left(i+\tfrac{1}{2}, j-\tfrac{1}{2}\right)\right] \end{aligned} \tag{5}$$

$$\begin{aligned} E_y^{n+(1/2)}&\left(i, j+\tfrac{1}{2}\right) \\ &= \alpha_y^e\left(i, j+\tfrac{1}{2}\right) E_y^n\left(i, j+\tfrac{1}{2}\right) - \beta_y^e\left(i, j+\tfrac{1}{2}\right) \\ &\quad \cdot \left[H_{zx}^{n+(1/2)}\left(i+\tfrac{1}{2}, j+\tfrac{1}{2}\right) - H_{zx}^{n+(1/2)}\left(i-\tfrac{1}{2}, j+\tfrac{1}{2}\right)\right. \\ &\quad \left. + H_{zy}^{n+(1/2)}\left(i+\tfrac{1}{2}, j+\tfrac{1}{2}\right) - H_{zy}^{n+(1/2)}\left(i-\tfrac{1}{2}, j+\tfrac{1}{2}\right)\right] \end{aligned} \tag{6}$$

$$\begin{aligned} H_{zx}^{n+(1/2)}&\left(i+\tfrac{1}{2}, j+\tfrac{1}{2}\right) \\ &= \alpha_x^h\left(i+\tfrac{1}{2}, j+\tfrac{1}{2}\right) H_{zx}^n\left(i+\tfrac{1}{2}, j+\tfrac{1}{2}\right) - \beta_x^h\left(i+\tfrac{1}{2}, j+\tfrac{1}{2}\right) \\ &\quad \cdot \left[E_y^{n+(1/2)}\left(i+1, j+\tfrac{1}{2}\right) - E_y^{n+(1/2)}\left(i, j+\tfrac{1}{2}\right)\right] \end{aligned} \tag{7}$$

$$\begin{aligned} H_{zy}^{n+(1/2)}&\left(i+\tfrac{1}{2}, j+\tfrac{1}{2}\right) \\ &= \alpha_y^h\left(i+\tfrac{1}{2}, j+\tfrac{1}{2}\right) H_{zy}^n\left(i+\tfrac{1}{2}, j+\tfrac{1}{2}\right) + \beta_y^h\left(i+\tfrac{1}{2}, j+\tfrac{1}{2}\right) \\ &\quad \cdot \left[E_x^n\left(i+\tfrac{1}{2}, j+1\right) - E_x^n\left(i+\tfrac{1}{2}, j\right)\right] \end{aligned} \tag{8}$$

where the superscripts denote time steps. The eight coefficients α_x^e, α_y^e, α_x^h, α_y^h, β_x^e, β_y^e, β_x^h, and β_y^h depend on the local PML conductivities σ_x or σ_y, as made explicit in the next section. Substituting (5), (7), and (8) into (6), an implicit update for E_y is obtained

$$\begin{aligned} &\beta_x^h\left(i+\tfrac{1}{2}, j+\tfrac{1}{2}\right) E_y^{n+(1/2)}\left(i+1, j+\tfrac{1}{2}\right) - c_1^1 E_y^{n+(1/2)}\left(i, j+\tfrac{1}{2}\right) \\ &\quad + \beta_x^h\left(i-\tfrac{1}{2}, j+\tfrac{1}{2}\right) E_y^{n+(1/2)}\left(i-1, j+\tfrac{1}{2}\right) \\ &\quad = c_2^1 E_y^n\left(i, j+\tfrac{1}{2}\right) + \left[\alpha_x^h\left(i+\tfrac{1}{2}, j+\tfrac{1}{2}\right) H_{zx}^n\left(i+\tfrac{1}{2}, j+\tfrac{1}{2}\right)\right. \\ &\quad - \alpha_x^h\left(i-\tfrac{1}{2}, j+\tfrac{1}{2}\right) H_{zx}^n\left(i-\tfrac{1}{2}, j+\tfrac{1}{2}\right) \\ &\quad + \alpha_y^h\left(i+\tfrac{1}{2}, j+\tfrac{1}{2}\right) H_{zy}^n\left(i+\tfrac{1}{2}, j+\tfrac{1}{2}\right) \\ &\quad \left. - \alpha_y^h\left(i-\tfrac{1}{2}, j+\tfrac{1}{2}\right) H_{zy}^n\left(i-\tfrac{1}{2}, j+\tfrac{1}{2}\right)\right] \end{aligned}$$

Manuscript received June 10,2002; revised August 13, 2002. The review of this letter was arranged by Associate Editor Dr. Ruediger Vahldieck.

The authors are with the ElectroScience Laboratory and Department of Electrical Engineering, The Ohio State University, Columbus, OH 43212 USA (e-mail: wangs@ee.eng.ohio-state.edu).

Digital Object Identifier 10.1109/LMWC.2003.808705

$$- \left\{\beta_y^h \left(i-\tfrac{1}{2}, j+\tfrac{1}{2}\right) \left[E_x^n \left(i-\tfrac{1}{2}, j+1\right) - E_x^n \left(i-\tfrac{1}{2}, j\right)\right] - \beta_y^h \left(i+\tfrac{1}{2}, j+\tfrac{1}{2}\right) \left[E_x^n \left(i+\tfrac{1}{2}, j+1\right) - E_x^n \left(i+\tfrac{1}{2}, j\right)\right]\right\} \tag{9}$$

with

$$c_1^1 = \frac{1}{\beta_y^e \left(i, j+\frac{1}{2}\right)} + \beta_x^h \left(i+\frac{1}{2}, j+\frac{1}{2}\right) + \beta_x^h \left(i-\tfrac{1}{2}, j+\tfrac{1}{2}\right)$$

$$c_2^1 = -\frac{\alpha_y^e \left(i, j+\frac{1}{2}\right)}{\beta_y^e \left(i, j+\frac{1}{2}\right)}$$

where it is clear that the left-hand side (LHS) of (9) forms a tridiagonal matrix, and the associated linear system can be solved with $\mathcal{O}(N)$ complexity [1].

In the second sub-step, the fields at the $(n+1)$ time step are obtained. The discretized equations are [2], [9]

$$\begin{aligned}
&\beta_y^h \left(i+\tfrac{1}{2}, j+\tfrac{1}{2}\right) E_x^{n+1} \left(i+\tfrac{1}{2}, j+1\right) - c_1^2 E_x^{n+1} \left(i+\tfrac{1}{2}, j\right) \\
&\quad + \beta_y^h \left(i+\tfrac{1}{2}, j-\tfrac{1}{2}\right) E_x^{n+1} \left(i+\tfrac{1}{2}, j-1\right) \\
&= c_2^2 E_x^{n+(1/2)} \left(i+\tfrac{1}{2}, j\right) \\
&\quad - \Big[\alpha_x^h \left(i+\tfrac{1}{2}, j+\tfrac{1}{2}\right) H_{zx}^{n+(1/2)} \left(i+\tfrac{1}{2}, j+\tfrac{1}{2}\right) \\
&\qquad - \alpha_x^h \left(i+\tfrac{1}{2}, j-\tfrac{1}{2}\right) H_{zx}^{n+(1/2)} \left(i+\tfrac{1}{2}, j-\tfrac{1}{2}\right) \\
&\qquad + \alpha_y^h \left(i+\tfrac{1}{2}, j+\tfrac{1}{2}\right) H_{zy}^{n+(1/2)} \left(i+\tfrac{1}{2}, j+\tfrac{1}{2}\right) \\
&\qquad - \alpha_y^h \left(i+\tfrac{1}{2}, j-\tfrac{1}{2}\right) H_{zy}^{n+(1/2)} \left(i+\tfrac{1}{2}, j-\tfrac{1}{2}\right)\Big] \\
&\quad - \Big\{\beta_x^h \left(i+\tfrac{1}{2}, j-\tfrac{1}{2}\right) \Big[E_y^{n+(1/2)} \left(i+1, j-\tfrac{1}{2}\right) \\
&\qquad - E_y^{n+(1/2)} \left(i, j-\tfrac{1}{2}\right)\Big] - \beta_x^h \left(i+\tfrac{1}{2}, j+\tfrac{1}{2}\right) \\
&\qquad \cdot \Big[E_y^{n+(1/2)} \left(i+1, j+\tfrac{1}{2}\right) - E_y^{n+(1/2)} \left(i, j+\tfrac{1}{2}\right)\Big]\Big\}
\end{aligned} \tag{10}$$

with

$$c_1^2 = \frac{1}{\beta_x^e \left(i+\frac{1}{2}, j\right)} + \beta_y^h \left(i+\frac{1}{2}, j+\frac{1}{2}\right) + \beta_y^h \left(i+\tfrac{1}{2}, j-\tfrac{1}{2}\right)$$

$$c_2^2 = -\frac{\alpha_x^e \left(i+\frac{1}{2}, j\right)}{\beta_x^e \left(i+\frac{1}{2}, j\right)}.$$

III. PML Implementations for ADI-FDTD

A. Traditional Scheme

In the usual PML implementation for the ADI-FDTD [9], the coefficients α_x^e, α_y^e, α_x^h, α_y^h, β_x^e, β_y^e, β_x^h, and β_y^h are written as

$$\begin{aligned}
\alpha_x^e &= \left(\frac{2\epsilon_0}{\Delta t} - \frac{\sigma_y}{2}\right) \Big/ \left(\frac{2\epsilon_0}{\Delta t} + \frac{\sigma_y}{2}\right) \\
\beta_x^e &= \left[\left(\frac{2\epsilon_0}{\Delta t} + \frac{\sigma_y}{2}\right) \Delta h\right]^{-1} \\
\alpha_y^e &= \left(\frac{2\epsilon_0}{\Delta t} - \frac{\sigma_x}{2}\right) \Big/ \left(\frac{2\epsilon_0}{\Delta t} + \frac{\sigma_x}{2}\right) \\
\beta_y^e &= \left[\left(\frac{2\epsilon_0}{\Delta t} + \frac{\sigma_x}{2}\right) \Delta h\right]^{-1} \\
\alpha_x^h &= \left(\frac{2\epsilon_0}{\Delta t} - \frac{\sigma_x}{2}\right) \Big/ \left(\frac{2\epsilon_0}{\Delta t} + \frac{\sigma_x}{2}\right) \\
\beta_x^h &= \left[\left(\frac{2\mu_0}{\Delta t} + \frac{\sigma_x \eta_0^2}{2}\right) \Delta h\right]^{-1} \\
\alpha_y^h &= \left(\frac{2\epsilon_0}{\Delta t} - \frac{\sigma_y}{2}\right) \Big/ \left(\frac{2\epsilon_0}{\Delta t} + \frac{\sigma_y}{2}\right) \\
\beta_y^h &= \left[\left(\frac{2\mu_0}{\Delta t} + \frac{\sigma_y \eta_0^2}{2}\right) \Delta h\right]^{-1}
\end{aligned} \tag{11}$$

where $\eta_0 = \sqrt{\mu_0/\epsilon_0}$, Δt is the time step and Δh is the cell size. These coefficients are obtained by assuming a central differencing approximation in time for the LHS involving the conduction terms in (1)–(4).

We simulate the radiation of a point source in free space using this algorithm. The whole computation domain, including the PML region, contains 42 $\times$ 42 cells with an uniform cell size equal to 1.33 mm. Ten layers of PML are used in both x and y directions with a conductivity profile [5] given by

$$\sigma = \frac{\sigma_{\max} |l - l_0|^4}{\delta^4}$$

where δ is the thickness of the PML absorber and l_0 represents the interface to free space. The conductivity $\sigma_{\max}$ is determined as in [9]. The excitation is located at the center of the computation region. The observation point is located ten cells away from the source and one cell away from the PML interface. The source is differentiated Gaussian pulse with both central frequency and half bandwidth equal to 3.175 GHz, applied to the H_z component. Fig. 1 shows the reflection error from the PML, defined as

$$R = 20 \log_{10} \left(\frac{|H^t - H_{ref}^t|}{\max |H_{ref}^t|}\right)$$

where χ is the Courant number defined by $\Delta t = \chi \Delta h / (\sqrt{2}\, v_p)$, and v_p is the phase velocity. H_{ref}^t in the equation above is the reference value calculated in a grid large enough so that any reflection from the boundary is causally isolated.

From Fig. 1, we observe that for small Courant numbers, the PML works well and the largest reflection error is about -75 dB. However, for large Courant numbers, the performance gets progressively worse. For $\chi = 6$, the largest reflection error is about -35 dB. This agrees with previous findings reported in [9].

B. Proposed Scheme

In the improved PML implementation, either forward or backward differencing approximation is used instead for the LHS of (1)–(4) in order to be collocated in time with their respective RHS. In the first sub-step, the following set of coefficients is used:

$$\begin{aligned}
\alpha_x^e &= (2\epsilon_0 - \sigma_y \Delta t)/2\epsilon_0 & \beta_x^e &= \Delta t/(2\epsilon_0 \Delta h) \\
\alpha_y^e &= 2\epsilon_0/(2\epsilon_0 + \sigma_x \Delta t) & \beta_y^e &= \Delta t/[(2\epsilon_0 + \sigma_x \Delta t)\Delta h] \\
\alpha_x^h &= 2\epsilon_0/(2\epsilon_0 + \sigma_x \Delta t) & \beta_x^h &= \Delta t/[(2\mu_0 + \sigma_x \eta_0^2 \Delta t)\Delta h] \\
\alpha_y^h &= (2\epsilon_0 - \sigma_y \Delta t)/2\epsilon_0 & \beta_y^h &= \Delta t/(2\mu_0 \Delta h).
\end{aligned} \tag{12}$$

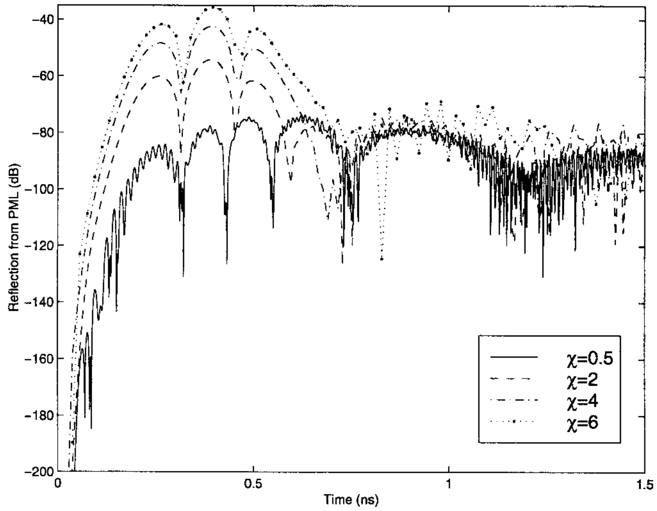

Fig. 1. Reflection error from the PML-ADI-FDTD method with the usual PML implementation.

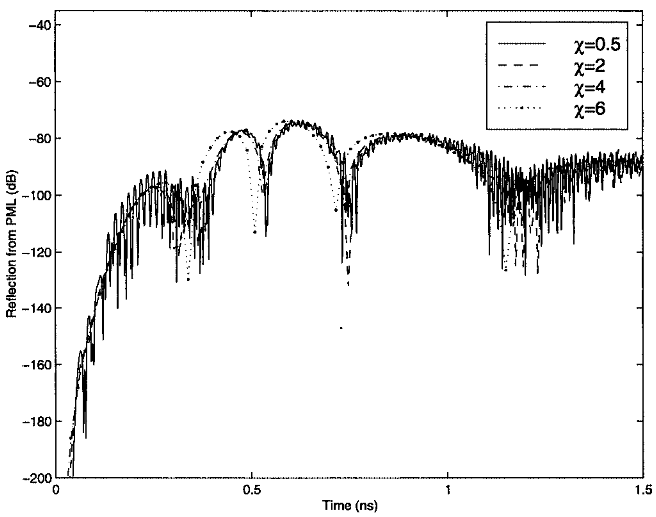

Fig. 2. Reflection error from the PML-ADI-FDTD method with the improved PML implementation.

In the second substep, a different set of coefficients is used

$$\begin{aligned}\alpha_x^e &= 2\epsilon_0/(2\epsilon_0+\sigma_y\Delta t) & \beta_x^e &= \Delta t/[(2\epsilon_0+\sigma_y\Delta t)\Delta h]\\ \alpha_y^e &= (2\epsilon_0-\sigma_x\Delta t)/2\epsilon_0 & \beta_y^e &= \Delta t/(2\epsilon_0\Delta h)\\ \alpha_x^h &= (2\epsilon_0-\sigma_x\Delta t)/2\epsilon_0 & \beta_x^h &= \Delta t/(2\mu_0\Delta h)\\ \alpha_y^h &= 2\epsilon_0/(2\epsilon_0+\sigma_y\Delta t) & \beta_y^h &= \Delta t/[(2\mu_0+\sigma_y\eta_0^2\Delta t)\Delta h].\end{aligned} \tag{13}$$

Fig. 2 shows the relative reflection error from this proposed PML from the same problem as before. We observe that the proposed new PML has a similar performance as the traditional one for small Courant numbers and it barely deteriorates for large Courant numbers. In particular, an improvement of more than 40 dB in the maximum reflection error is obtained for Courant factor $\chi = 6$, compared to Fig. 1.

For this spatial cell size, proper care should be exercised when interpreting results for even larger Courant numbers. In the example above, the reflection can reach -60 dB with $\chi = 10$ and other parameters being the same. This is not caused by a larger χ *per se*, but instead because the resulting time step Δt is closer to the Nyquist limit of the source pulse and increasingly larger than the average relaxation time inside the PML. By decreasing the cell size Δh, about the same reflection level as in Fig. 2 could be achieved with $\chi = 10$, provided that the same physical PML thickness is used. It should also be pointed out that the truncation error of the ADI-FDTD is $\mathcal{O}(\Delta t^2)$ [1], [4].

Finally, we have also tested the implementation of PML–ADI-FDTD schemes with exponential differencing in time [5], but did not observe any significant improvement in the PML performance (the largest reduction on the reflection error in our tests was at $\chi = 6$ and within 3 dB).

IV. Conclusion

In this letter, we have introduced an improved implementation of the PML absorbing boundary condition for the ADI-FDTD method. The proposed PML relies on successively applying forward and backward differencing in time for the conduction terms in the ADI-FDTD update. Compared to the traditional PML implementation, the performance of the proposed PML is more efficient for large Courant numbers.

References

[1] J. C. Strikwerda, *Finite Difference Schemes and Partial Differential Equations*. New York: Chapman & Hall, 1989.

[2] T. Namiki, "A new FDTD algorithm based on alternating-direction implicit method," *IEEE Trans. Microwave Theory Tech.*, vol. 47, pp. 2003–2007, Oct. 1999.

[3] F. Zheng, Z. Chen, and J. Zhang, "A finite-difference time-domain method without the Courant stability conditions," *IEEE Microwave Guided Wave Lett.*, vol. 9, pp. 441–443, Nov. 1999.

[4] S. G. García, T.-W. Lee, and S. C. Hagness, "On the accuracy of the ADI-FDTD method," *IEEE Antennas Wireless Propagat. Lett.*, vol. 1, pp. 31–34, Feb. 2002.

[5] J. P. Berenger, "A perfectly matched layer for the absorption of electromagnetic waves," *J. Comput. Phys.*, vol. 114, pp. 185–200, Oct. 1994.

[6] S. D. Gedney, "An anisotropic PML absorbing media for the FDTD simulation of fields in lossy and dispersive media," *Electromagnetics*, vol. 16, pp. 399–415, Jul.–Aug. 1996.

[7] Z. S. Sacks, D. M. Kingsland, R. Lee, and J. F. Lee, "A perfectly matched anisotropic absorber for use as an absorbing boundary condition," *IEEE Trans. Antennas Propagat.*, vol. 43, pp. 1460–1463, Dec. 1995.

[8] F. L. Teixeira and W. C. Chew, "General closed-form PML constitutive tensors to match arbitrary bianisotropic and dispersive linear media," *IEEE Microwave Guided Wave Lett.*, vol. 8, pp. 223–225, June 1998.

[9] G. Liu and S. D. Gedney, "Perfectly matched layer media for an unconditionally stable three-dimensional ADI-FDTD method," *IEEE Microwave Guided Wave Lett.*, vol. 10, pp. 261–263, July 2000.